

## Fine monitoring of the effects of grapevine resistance loci on the development of *Plasmopara viticola*

Wiedemann-Merdinoglu S\*, Lacombe M.C., Dorne M.A., Dumas V., Onimus C., Prado E., Schneider C., Louise Dit Adèle S., Misbach J., Negrel L., Baltenweck R., Huguency P. and D. Merdinoglu

INRAE, Centre Grand Est-Colmar, 28 rue de Herrlisheim, 68000 Colmar, France

### 1 Introduction

*Plasmopara viticola*, the agent of downy mildew native to North America, was introduced into Europe in the second half of the 19<sup>th</sup> century. It rapidly devastated all the European vineyards (Gessler *et al.*, 2011). For decades, massive applications of fungicides were used to control downy mildew, because the European grapevine varieties display no or little resistance. In this context, the development of resistant varieties is a promising strategy for limiting the use of fungicides. Over the last twenty years, more than thirty genetic factors, derived mainly from *Vitis* species, have been identified and some of them are considered as major genes. The strategy of pyramiding resistance factors in a variety is used to limit the risk of resistance breakdown by pathogen isolates in the vineyard. In this strategy, the choice of different resistance genes to be combined together in the same variety is crucial to ensure resistance durability.

In this study, we analyzed the effect of four resistance factors on the *P. viticola* development: *Rpv1*, located on linkage group (LG) 12 and inherited from *V. rotundifolia* (Merdinoglu *et al.*, 2003); *Rpv3.1*, located on LG 18, inherited from *V. rupestris* (Welter *et al.*, 2007; Bellin *et al.*, 2009; Di Gaspero *et al.*, 2012; Foria *et al.*, 2020); *Rpv3.3* located on LG 18, inherited from *V. labrusca* or *V. riparia* (Di Gaspero *et al.*, 2012; Vezzulli *et al.* 2019) and *Rpv10* located on LG 9 and inherited from the Asian species *V. amurensis* (Schwander *et al.*, 2012). For this, we used a grapevine population in which the four resistance factors (loci) segregated. Among the fifteen possible combinations of these loci, the study focused only on the individual loci to analyse the effect of each of them compared to the susceptible genotype (with no resistance factor). For this purpose, three approaches were implemented: macroscopic symptoms assessment, cytological observations of developmental stages and monitoring of the pathogen biomass by quantification of *P. viticola*-specific lipids.

### 2 Materials and methods

**Plant material and experimental design.** For each *Rpv* locus, three genotypes were selected among the population and for each genotype, three plants were used. Plants, derived from green cuttings, were grown on potting soil in a greenhouse at 22-19°C (day-night) and a photoperiod of 16 h light until reaching a 12 leaf stage. For each plant, the leaves, number 4 and 5, (starting from the apex) were excised and transferred to the laboratory. Leaf discs (2 cm diameter) were produced. All the leaf discs were placed in 12 microwell plates. They were inoculated by spraying a sporangia solution ( $5 \times 10^4$  sp/ml<sup>-1</sup>) or with water. For each leaf, 5 discs were sprayed with the *P. viticola* “Colmar” isolate and 5 discs with the “Lednice” isolate. This isolate was able to overcome the *Rpv3.1* locus (Peressotti *et al.*,

2010). The remaining leaf discs were sprayed with water, as a control. Then, the plates were incubated in a growth

chamber (21°C, 80% relative humidity, 50 µmol/m<sup>2</sup>/s light intensity). Leaf discs were collected at 24, 48, 72, 96 hours and 6 days post infection. Each leaf disc was cut in 2 halves, one for the cytological study and one for the pathogen biomass assessment.

**Macroscopic symptoms assessment using the OIV 452-1 scale.** The symptoms present on the discs were observed at 4, 5 and 6 days post infection (dpi) under a Zeiss Stemi 508 stereomicroscope (Zeiss, Oberkochen, Germany) at 32 x magnification and were rated with the visual index OIV 452-1 scale, recommended by the Office International de la Vigne et du Vin (Anonymous 2009). Five categorical values from 1 (the most susceptible) to 9 (the most resistant) were assigned based on the absence or presence of necrotic reactions and their size, as well as on the extent of sporulating area (Bellin *et al.*, 2009).

**Cytological observations after aniline blue staining.** The pathogen development was monitored by cytological observations after aniline blue staining (Trouvelot *et al.*, 2008). Four developmental stages were observed: substomatal vesicle; long primary hypha; branched hypha and mycelium (Unger *et al.*, 2007; Diez-Navajas *et al.*, 2008). In addition, collapsed structures linked to long hypha, branched hypha and to mycelium, were also reported. The observations were made at 24, 48, 72 and 96 hours post infection. Discs were mounted on slides for fluorescence microscopy visualization using a Zeiss Axio Imager M2 (Zeiss, Oberkochen, Germany) with a Dapi filter and with 250 x magnification. For each half disc, 3 fields were observed and each pathogen structure was analyzed and scored. For each *Rpv* locus and for the susceptible genotypes (S), the results were presented as a relative frequency of each stage as described in Fig. 1.

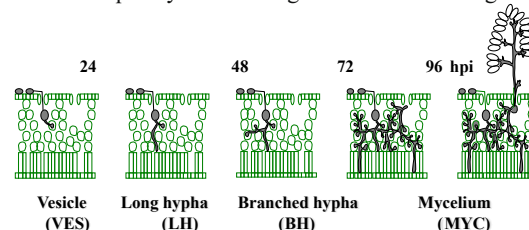


Figure 1: *P. viticola* structures according to development stages.

**Monitoring of the pathogen biomass by quantification of *P. viticola*-specific lipids.** The assessment of the pathogen biomass by relative quantification of *P. viticola* lipids (Negrel *et al.*, 2018), was monitored at 24, 48, 72 and 96 hours post infection. These lipids included ceramides and derivatives of arachidonic and eicosapentaenoic acid which were not detected in healthy grapevine plants. Prior to extraction, each leaf disc was freeze-dried, weighed and powdered. Metabolites were extracted with MeOH/CHCl<sub>3</sub>

Corresponding author: [sabine.wiedemann@inrae.fr](mailto:sabine.wiedemann@inrae.fr)

(1/1, v/v) using 15 µL per mg dry weight. The suspension of leaf powder in MeOH/CHCl<sub>3</sub> was then sonicated for 15min in an ultrasound bath. Two milliliters of ultrapure water were added to allow phase separation. After centrifugation at 15,000 g for 10 min, 100 µL of the chloroform phase was recovered, diluted with 100 µL of MeOH and analyzed by UHPLC-MS according to Negrel *et al.* (2018). The results were presented as the total lipids detected for each *Rpv* locus and for each *P. viticola* isolate, corresponding to the sum of peak areas resulting from individually quantified lipids.

### 3 Results

These four *Rpv* loci, showed different phenotypes of partial resistance (Merdinoglu *et al.*, 2018; Possamai *et al.*, 2020). General observations led us to consider the sporulation and the necrosis (hypersensitive reaction) as the principal components of the resistance. At 4 dpi, sporulation had emerged from the abaxial surface of all the inoculated leaf discs. At this time point, the phenotypes clearly revealed the different resistance features induced by the four *Rpv* loci.

#### Symptom assessments by using the OIV 452-1 scale.

With the “Colmar” isolate (Fig.2), sporulation was observed for all *Rpv* loci. However, the number of spores produced was variable. For the susceptible genotypes (S), the quantity of spores produced was the highest, whereas for the locus *Rpv10*, only very few spores were produced. In addition, a hypersensitive reaction (HR) was observed for all *Rpv* loci, however they displayed different HR characteristics in shape, size, color and number. The *Rpv3.1* and *Rpv10* loci developed very small necrosis, whereas *Rpv1* and *Rpv3.3* loci induced larger necrosis. For the genotypes with the *Rpv3.1* locus and challenged with the “Lednice” isolate (Fig.3), the sporulation level was as high as that of “S”. More generally, for the susceptible genotypes (S) and for each *Rpv* locus, the sporulation levels seemed higher with this isolate. The HR was also less visible.

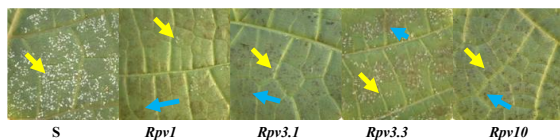


Figure 2: Phenotypes observed on the leaf discs surface with the different resistance loci (*Rpv*), 4 days post infection (dpi), challenged with the *P. viticola* isolate “Colmar”. Sporulation (yellow arrow), hypersensitive reaction or HR (blue arrow).

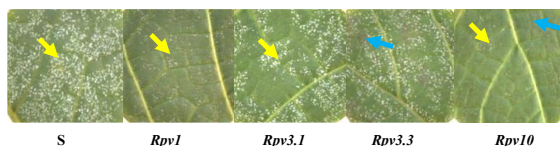


Figure 3: Phenotypes observed on the leaf discs surface with the different resistance loci (*Rpv*), 4 days post infection (dpi), challenged with the *P. viticola* isolate “Lednice”. Sporulation (yellow arrow), hypersensitive reaction or HR (blue arrow).

The analysis of the OIV452-1 scores (Fig.4) showed that with the “Colmar” isolate, all *Rpv* loci induced a partial

resistance displaying scores between 4.5 (*Rpv* 3.3) and 7.7 for *Rpv10*. The scores of “S” and that of *Rpv3.3* locus were very close (between 3.2 and 4.0). The scores of the *Rpv1* and the *Rpv3.1* loci were very similar, but below that of the *Rpv10* locus. With the “Lednice” isolate, the OIV452-1 scores of all *Rpv* loci were lower compared to those produced by the other isolate, especially for the *Rpv3.1* locus, whose score dropped from 6.8 to 3.7 and reached that of “S”.

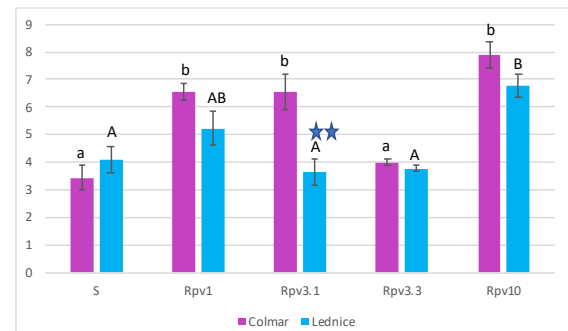


Figure 4: OIV452-1 scores observed with the different *Rpv* loci and the susceptible genotypes (S), 4 days post infection (dpi) challenged with the *P. viticola* “Colmar” and “Lednice” isolates. The scores from 1 to 4 were considered to be representative of susceptible phenotypes. All the scores > 4 were considered to represent resistant phenotypes. A score of 9, reflected a total resistance. Letters indicate statistically different scores among *Rpv* loci, obtained by pairwise comparisons (Tukey method). Bars indicate standard errors.

#### Cytological analysis of the P. viticola development.

With the “Colmar” isolate (Fig.5), the “mycelium” appeared as the most important structure for the “S”, even if “branched hypha” and “collapsed hypha” or “collapsed mycelium” were sometimes observed. The same profile was observed for the *Rpv3.3* locus but with a higher percentage of “branched hypha”. This suggests that for this locus, the pathogen development was slightly delayed. For the *Rpv1*, *Rpv3.1* and *Rpv10* loci, “collapsed branched hypha” was the most prevalent stage, suggesting an early destruction of the pathogen structures, especially for the *Rpv10* locus for which “collapsed long hypha” were also observed.

With the “Lednice” isolate (Fig.6), the observed profiles were similar to that of the “Colmar” isolate, except for the *Rpv3.3* locus. In this case, the profile was close to that of the “S” and no collapsed structures or delay in the pathogen development were observed. Interestingly, for the *Rpv1* and *Rpv3.3* loci, the proportion of mycelium was higher than for the “Colmar” isolate, suggesting that “Lednice” was more aggressive than the “Colmar” isolate. For the *Rpv10* locus, no differences between isolates were observed.

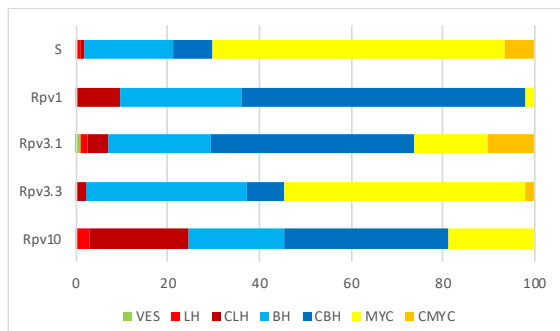


Figure 5: Percentage of each pathogen stage observed for the susceptible genotypes (S) and for the genotypes with each *Rpv* locus inoculated with the *P. viticola* “Colmar” isolate. VES: vesicle, LH: long hypha, CLH: collapsed long hypha. BH: branched hypha. CBH: collapsed branched hypha. MYC: mycelium. CMYC: collapsed mycelium.

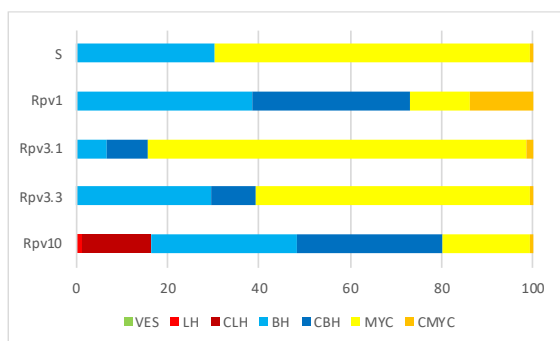


Figure 6: Percentage of each pathogen stage observed for the susceptible genotypes (S) and for the genotypes with each *Rpv* locus inoculated with the *P. viticola* “Lednice” isolate. VES: vesicle, LH: long hypha, CLH: collapsed long hypha. BH: branched hypha. CBH: collapsed branched hypha. MYC: mycelium. CMYC: collapsed mycelium.

Evaluation of the pathogen biomass by quantification of pathogen-specific lipids (Fig.7). With the “Colmar” isolate, the highest amount of total lipids was obtained for the “S” genotypes and for the *Rpv3.3* locus. Conversely, the lowest amount was detected for the *Rpv10* locus (20 times less than for the “S”). The amount detected for *Rpv1* and *Rpv3.1* loci was respectively 11 and 8 times lower than for the “S”. For all the *Rpv* loci, the total lipid amounts were higher with “Lednice” than with the “Colmar” isolate. A significant isolate effect was detected for the *Rpv3.1* locus for which the amount measured was close to that of the “S”. Interestingly, a significant effect was also observed for the *Rpv1* locus.

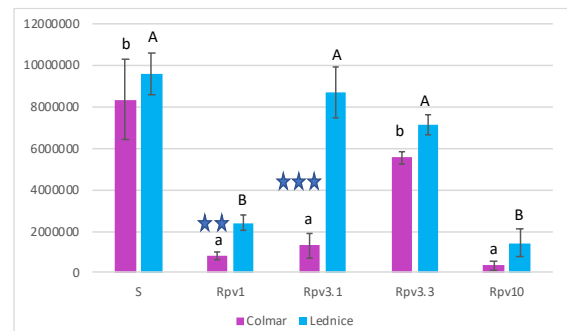


Figure 7: Peak area (arbitrary units) of *P. viticola* lipids quantified for the susceptible genotypes (S) and for the genotypes with each *Rpv* locus inoculated with the *P. viticola* “Colmar” and “Lednice” isolates. Letters indicate statistically different values among *Rpv* loci, obtained by pairwise comparisons (Tukey method). Bars indicate standard errors.

#### 4 Discussion

In this study, the first sporulation events were observed at 4 dpi for “S” and for all *Rpv* genotypes, albeit with different intensity. Sporulation levels ranged from high for “S” and *Rpv3.3* to very low for *Rpv10*, with both pathogen isolates. *Rpv1* and *Rpv3.1* loci exhibited intermediate levels with the “Colmar” isolate, whereas sporulation of the “Lednice” isolate was higher with the *Rpv3.1* locus, due to the breakdown of this locus by this isolate. According to Bellin et al, (2009), the OIV 452-1 scale rated the plant reaction represented by the necrosis pattern (flecks, spots, substomatal HR) and the sporulation level. The OIV 452-1 scores clearly reflected the symptoms induced by the different *Rpv* loci. However, this approach didn’t explain how these symptoms were produced. Generally, symptoms are the result of the mesophyll colonization by the pathogen and the plant reaction effect. The colonization is considered as a sequence of transformations of pathogen structures: from vesicles to mycelium. At 4 dpi, both the cytology and the pathogen biomass approaches indicated a delay of the pathogen development between the *Rpv* genotypes and the susceptible genotypes “S”. The pathogen biomass approach demonstrated that for *Rpv1*, *Rpv3.1* and *Rpv10* loci, the total amount of pathogen lipids was respectively 11, 8 and 20 times lower than for the “S” genotypes. This indicated that the pathogen development was strongly reduced by the presence of these *Rpv* loci but with different degrees. Moreover, the cytological approach revealed that pathogen structures were collapsed or destroyed by the presence of these loci at different time points of the pathogen development. For the *Rpv10* locus, the collapsed “long hypha” stage represented 20% of the total structures observed. This indicated a rapid effect of this resistance locus after the beginning of the infection. For the *Rpv1* locus, 60% of the pathogen structures were represented by the “collapsed branched hypha” stage, suggesting that the effect was delayed compared to that of *Rpv10*. The destruction of the pathogen structures could be the result of the defense mechanisms effect. Several recent transcriptomic studies have shown that *Rpv* loci are able to induce multiple defense responses. The accumulation of stilbenes seems to be a common defense response between *Rpv1* (Qu et al, 2021), *Rpv3.1* (Eisenmann et al., 2019, Chitarrini et al., 2020 and Wingerter et al., 2021), *Rpv3.3* (Vezzulli et al., 2019) and for *Rpv10* (Fröbel et al., 2019).

The cytological and the pathogen biomass approaches seemed to be complementary to produce information concerning the effect of the *Rpv* loci studied either during the early stages of the pathogen development or for the explanation of the macroscopic symptoms.

## 5 Conclusions

This study showed, by observing the macroscopic symptoms, that the *Rpv1*, *Rpv3.1*, *Rpv3.3* and *Rpv10* loci induced various resistance levels to *P. viticola*. The high resistance level conferred by the *Rpv10* locus could be explained by a delay and a strong inhibition of the pathogen development associated to a rapid destruction of the pathogen. The *Rpv1* and *Rpv3.1* loci conferred an intermediate effect with very close features, except in the presence of a virulent pathogen isolate for the *Rpv3.1* locus. The effect induced by the presence of the *Rpv3.3* locus is weak compared to that of the other loci.

## References

1. Bellin D., Peressotti E., Merdinoglu D., Wiedemann-Merdinoglu S., Adam-Blondon A.F., Cipriani G., Morgante M., Testolin R. and Di Gaspero G. 2009. Resistance to *Plasmopara viticola* in grapevine 'Bianca' controlled by a major dominant gene causing localised necrosis at the infection site. *Theor Appl Genet*, 120:163–176.
2. Chitarrini G., Riccadonna S., Zulini L., Vecchione A., Stefanini M., Langer S., Pindo M., Cestaro A., Franceschi P., Magris G., Folia S., Morgante M., Di Gaspero G and Vrhovsek U. 2020. Two-omics data revealed commonalities and differences between Rpv12- and Rpv3-mediated resistance in grapevine. *Sci Rep*. 10:1–15.
3. Díez-Navajas A-M., Wiedemann-Merdinoglu S., Greif C and Merdinoglu D. 2008. Nonhost versus host resistance to the grapevine downy mildew, *Plasmopara viticola*, studied at the tissue level. *Phytopathology* 98:776–780.
4. Di Gaspero G., Cipriani G., Adam-Blondon A.F. and Testolin R. 2007. Linkage maps of grapevine displaying the chromosomal locations of 420 microsatellite markers and 82 markers for R gene candidates. *Theor Appl Genet*, 114:1249-1263.
5. Eisenmann B., Czermel S., Ziegler T., Buchholz G., Kortekamp A., Trapp O., Rausch T., Dry I and Bogs J. 2019. Rpv3-1 mediated resistance to grapevine downy mildew is associated with specific host transcriptional responses and the accumulation of stilbenes. *BMC Plant Biol*, 19:1–17.
6. Folia S., Copetti D., Eisenmann B., Magris G., Michele Vidotto M., Scalabrin S., Testolin R., Cipriani G., Wiedemann-Merdinoglu S., Jochen Bogs J., Di Gaspero G. and Morgante M. 2020. Gene duplication and transposition of mobile elements drive evolution of the Rpv3 resistance locus in grapevine. *The Plant Journal*, **101**:529-542
7. Fröbel S., Dudenhöffer J., Töpfer R. and Zyprian, E. 2019. Transcriptome analysis of early downy mildew (*Plasmopara viticola*) defense in grapevines carrying the Asian resistance locus *Rpv10*. *Euphytica*, 215:28
8. Gessler C., Pertot, I., Perazzolli M. 2011: *Plasmopara viticola*: a review of knowledge on downy mildew of grapevine and effective disease management. *Phytopathol. Mediterr.*, 50:3-44.
9. Merdinoglu D., Wiedemann-Merdinoglu S., Coste P., Dumas V., Haetty S., Butterlin G. and Greif C. 2003. Genetic analysis of downy mildew resistance derived from *Muscadinia rotundifolia*. *Acta Horti*, 603:451–456. doi:10.17660/ActaHortic. 2003.603.57.
10. Merdinoglu D., Schneider C., Prado E., Wiedemann-Merdinoglu S. and Mestre P. 2018. Breeding for durable resistance to downy and powdery mildew in grapevine. *OENO One*, 52 :189-195
11. Negrel L., Halter D., Wiedemann-Merdinoglu S., Rustenholz C., Merdinoglu D., Huguency P. and Baltenweck R. 2018. Identification of lipid markers of *Plasmopara viticola* infection in grapevine using non targeted metabolomic approach. *Front. Plant Sci*, 9:360.
12. OIV. Descriptor List for Grape Varieties and Vitis Species, 2nd ed.; Office International de la Vigne et du Vin: Paris, France, 2009
13. Peressotti E., Wiedemann-Merdinoglu S., Delmotte F., Bellin D., Di Gaspero G., Testolin R., Merdinoglu D. and Mestre P. (2010). Breakdown of resistance to grapevine downy mildew upon limited deployment of a resistant variety. *Plants*, 9:781.
14. Possamai T., Migliaro D., Gardiman M., Velasco R. and de Nardi B. 2020. Rpv mediated defense responses in grapevine offspring resistant to *Plasmopara viticola*. *BMC Plant Biology*, 21:528.
15. Qu J., Dry I., Liu L., Guo Z, and L. Yin. 2021. Transcriptional profiling reveals multiple defense responses in downy mildew-resistant transgenic grapevine expressing a TIR-NBS-LRR gene located at the MrRUN1/MrRPV1 locus. *Horticultural Research*, 8:161
16. Schwander F., Eibach R., Fechter I., Hausmann L., Zyprian E. and Töpfer R. 2012. *Rpv10*: a new locus from the Asian *Vitis* gene pool for pyramiding downy mildew resistance loci in grapevine. *Theor Appl Genet*, 124:163–176.
17. Trouvelot S., Varnier A-L., Allègre M., Mercier L., Baillieux F., Arnould C., Gianinazzi-Pearson V., Klarzynski O., Joubert J-M., A. Pugin A., and Daire X. 2008. A  $\beta$ -1,3 glucan sulfate induces resistance in grapevine against *Plasmopara viticola* through priming of defense responses, including HR-like cell death. *MPMI* 21:232-243.
18. Unger S., Büche C., Boso S. and Kassemeyer H.-H. 2007. The course of colonization of two different Vitis genotypes by *Plasmopara viticola* indicates compatible and incompatible host-pathogen interactions. *Phytopathology*, 97:780–786.
19. Vezzulli S., Malacarne G., Masuero D., Vecchione A., Dolzani C., Goremykin V., Mehari Z-H., Banchi E., Velasco R., Stefanini M., Vrhovsek U., Zulini L., Franceschi P., and Moser C. 2019. The *Rpv3-3* haplotype and stilbenoid induction mediate downy mildew resistance in a grapevine interspecific population. *Front. Plant Sci*, **10**:234.
20. Welter L.J, Göktürk-Baydar N., Akkurt M., Maul E., Eibach R., Töpfer R. and Zyprian E. 2007. Genetic mapping and localization of quantitative trait loci affecting fungal disease resistance and leaf morphology in grapevine (*Vitis vinifera* L). *Mol Breed*, 20:359–374.
21. Wingerter C., Eisenmann B., Weber P., Dry I and Bogs J. 2021. Grapevine Rpv3-, Rpv10- and Rpv12-mediated defense responses against *Plasmopara*

- viticola* and the impact of their deployment on fungicide use in viticulture. *BMC Plant Biol*, 21:470.
22. Zyprian E., Ochßner I., Schwander F., Simon S., Hausmann L., Bonow-Rex M., Moreno-Sanz P., Grando M.S., Wiedemann-Merdinoglu S., Merdinoglu D., Eibach R. and Töpfer R. 2016. Quantitative trait loci affecting pathogen resistance and ripening of grapevines. *Mol Genet Genomics*, 291:1573–1594.